第 33 卷第 12 期
2017 年 12 月

无 机 化 学 学 报
CHINESE JOURNAL OF INORGANIC CHEMISTRY

Vol.33 No.12
2193-2200

# 棒状 $CuFe_4O_x$ 的可控合成及其异戊醇脱氢反应的催化性能

马宏彬　马令娟*　侯梦宁　岳明波
(曲阜师范大学化学与化工学院,曲阜　273165)

**摘要**：利用液相沉淀法可控合成了均匀的棒状 $CuFe_4O_x$ 催化剂。通过原位 X 射线粉末衍射(XRD)、高分辨透射电子显微镜(TEM)及程序升温还原(TPR)等手段表征其晶相结构、形貌和还原性能。通过还原棒状 $CuFe_4O_x$ 获得 $Cu^0/Fe_3O_4$ 纳米棒,原位 X 射线光电子能谱(XPS)用于确定 $Cu^0/Fe_3O_4$ 表面的相组成。通过液相沉淀法制备棒状 $CuFe_4O_x$,在 120 ℃保持 3 h 后加入 $Na_2CO_3$ 溶液至 pH 等于 9 时所得棒状形貌最为规整。以异戊醇脱氢反应作为探针反应,比较了 $Cu^0/Fe_3O_4$ 纳米棒和 $Cu^0/Fe_3O_4$ 纳米颗粒的催化反应性能,发现 $Cu^0/Fe_3O_4$ 纳米棒比 $Cu^0/Fe_3O_4$ 纳米粒子具有更好的活性和稳定性,表明棒状 $Fe_3O_4$ 担载的 Cu 纳米粒子具有更好的结构稳定性。

**关键词**：$CuFe_4O_x$ 复合物；XPS；异戊醇脱氢
**中图分类号**：O643.32；O614.121　　**文献标识码**：A　　**文章编号**：1001-4861(2017)12-2193-08
**DOI**：10.11862/CJIC.2017.275

## Rod-like $CuFe_4O_x$ Composite: Controllable Synthesis and Catalytic Performance in Isoamylic Alcohol Dehydrogenation

MA Hong-Bin　MA Ling-Juan*　HOU Meng-Ning　YUE Ming-Bo
(*School of Chemistry and Chemical Engineering, Qufu Normal University, Qufu, Shandong* 273165, *China*)

**Abstract:** Uniformly rod-shaped $CuFe_4O_x$ catalysts were controllably fabricated through a liquid-phase precipitation method. The phase structure, morphology and reduction properties of the catalyst were characterized by *in-situ* powder X-ray diffraction (XRD), high resolution transmission electron microscope (HRTEM) and temperature-programmed reduction (TPR). $Cu^0/Fe_3O_4$-nanorod obtained from the reduction of rod-shaped $CuFe_4O_x$ structure and the surface phase composition of $Cu^0/Fe_3O_4$ was detailed studied by *in-situ* X-ray photoelectron spectroscopy (XPS). $CuFe_4O_x$ composites with rod-shape were prepared by an aqueous precipitation method that means after stirring time at 120 ℃ for 3 h, $Na_2CO_3$ solution was added until pH value equal to 9. In this case, the most uniform $CuFe_4O_x$ composites with rod-shape were obtained. $Cu^0/Fe_3O_4$-nanorod catalyst presents higher activity and stability for the dehydrogenation of isoamylic alcohol than $Cu/Fe_3O_4$-nanoparticles, due to $Cu^0$ nanoparticles supported on the rod-shaped $Fe_3O_4$ exhibits higher structure stability.

**Keywords:** $CuFe_4O_x$ composite; XPS; dehydrogenation of isoamylic alcohol

## 0 Introduction

Morphology-dependent nanocatalysts have been intensively explored over metal and metal oxides[1-3], but less attention has been paid to binary metal oxides and oxide-supported metals. Copper-based catalysts are extensively studied due to their good catalytic performance in many industrial reactions

收稿日期:2017-07-12。收修改稿日期:2017-09-22。
国家自然科学基金(No.21403124)和山东省自然科学基金(No.ZR2014JL014,ZR2014BM012)资助项目。
*通信联系人。E-mail:malingjuan@qfnu.edu.cn

such as methanol synthesis and water gas shift reactions[4-6]. And, $Cu/Fe_3O_4$ catalysts are one of the most effective catalysts and their catalytic properties strongly depended on the properties of $Fe_3O_4$ particles[7]. The major drawbacks of Cu-based catalyst are still the difficulties of homogeneous dispersion of Cu particles on supports and poor thermal stability[8]. Yang et al. proposed a space-confined synthesis method to prepare rod-shaped $CuFe_2O_4$ which was reduced to $Cu/Fe_3O_4$ catalyst with fine $Cu^0$ nanoparticles supported on $Fe_3O_4$ rod[9]. Additionally, the precursors of copper are also very important for the stability and activity of copper species. Kameoka et al.[10] proposed that spinel $CuFe_2O_4$ was an effective precursor for a high performance copper catalyst which showed high thermal stability and activity. However, Cu content in stoichiometric $CuFe_2O_4$ is too high to be dispersed on the surface of $Fe_3O_4$ support. As a result, controllable synthesized rod-shaped $CuFe_4O_x$ was used as the precursor of $Cu/Fe_3O_4$ and the composition of reduced product are well studied.

It is also known that copper-based catalysts show high activity in the dehydrogenation of alcohols [11]. Isovaleraldehyde is an important industrial intermediary in the manufacturing of synthetic resins, special chemicals and isovaleric acid which is widely used in the medical industry and Shiau et al. indicated that Cu-based catalysts have a good activity for isoamylic alcohol dehydrogenation[12]. Crivello et al.[13] also studied the performance of Cr-Cu-Mg catalysts in the dehydrogenation of isoamylic alcohol. In this paper dehydrogenation of isoamylic alcohol was used to assess the catalytic performance of $Cu/Fe_3O_4$-nanorods and $Cu/Fe_3O_4$-nanoparticle was also prepared to compare the performance with $Cu/Fe_3O_4$-nanorods.

## 1 Experimental details

### 1.1 Catalyst preparation

All the chemicals were analytical grade and were used without further purification. The synthesis of $CuFe_4O_x$ composite with rod-shape was prepared by an aqueous precipitation method which was in accordance with the preparation of $\alpha$-$Fe_2O_3$ nanorods[14]. The typical synthesis procedure was described as follows. $CuCl_2\cdot 2H_2O$ (0.68 g), $FeCl_3\cdot 6H_2O$ (4.32 g), NaCl (11.60 g), and PEG (10 mL) were dissolved in 190 mL water and then the solution was gradually heated to 120 ℃ at vigorous stirring and stay at 120 ℃ for 3 h. A $Na_2CO_3$ aqueous solution (0.2 mol·L$^{-1}$) was added through a syringe pump at a rate of 1.0 mL·min$^{-1}$. The mixture was then aged at 120 ℃ for 1 h. The precipitate was washed with water and ethanol, and dried at 60 ℃ for 6 h. Finally, the dried sample was calcined at different temperature.

$CuFe_4O_x$ nanoparticles were prepared by co-precipitation method. An aqueous solution of $Cu(NO_3)_2\cdot 3H_2O$ (4 mmol) and $Fe(NO_3)_3\cdot 9H_2O$ (16 mmol) was rapidly added into 100 mL 0.5 mol·L$^{-1}$ $Na_2CO_3$ aqueous solution at room temperature. The obtained reddish brown precipitate was collected by filtration, washed with deionized water and ethanol, dried at 80 ℃ overnight and finally calcined at 500 ℃ for 10 h in air condition.

### 1.2 Characterization of samples

X-ray diffraction (XRD) pattern was performed on a RigakuD/MAX-RB diffractometer with Cu $K\alpha$ radiation ($\lambda$=0.154 nm) at $U$=40 kV and $I$=200 mA. Powder patterns of uncalcined precursor and catalysts obtained by calcined at different conditions were recorded in the $2\theta$ range of 15°~80° and the scan rate was 3°·min$^{-1}$. *In-situ* XRD were carried out in the $2\theta$ range of 15°~60° while a catalyst was in a reductive atmosphere (5%$H_2$ balanced with 95%He) with a scan rate of 5 ℃·min$^{-1}$ to track potential evolution of phase in the $H_2$ treatment. $N_2$ adsorption-desorption of sample was tested by Nova 4200e physical adsorption instrument.

The HRTEM images were gotten from the JEM-2010 and TEM images were examined using Hitachi 7700 transmission electron microscope. The X-ray photoelectron spectroscopy (XPS) was performed in an ultrahigh-vacuum chamber that has attached a high-pressure cell or batch reactor. The sample could be transferred between the reactor and vacuum chamber without exposure to air. Temperature-programmed reduction (TPR) experiments were performed in a

quartz tube micro-reactor connected to an Auto Chem 2920 instrument. The experiments were performed on 40 mg of catalyst under the flowing 5% $H_2$ balanced with $N_2$ (30 mL·min$^{-1}$) with a heating rate of 1 ℃·min$^{-1}$.

### 1.3 Catalytic activity

Catalytic activities of the $CuFe_4O_x$ nanoparticles and nanorods were carried out in a continuous flow type reactor with a fixed catalyst bed operated at atmospheric pressure. Isoamylic alcohol serves as reagent was introduced through $N_2$ gas. The $W/F_0$ is controlled to 41.3 $g_{catalyst}$·h·mol$^{-1}$. Only isoamylic alcohol, isovaleraldehyde and hydrogen were detected in the reaction, other products were found in trace amounts and will be neglected. Analysis of the feed and effluent gas were performed after water condensation by gas chromatograph (GC).

## 2 Results and discussion

### 2.1 Controllable synthesis of $CuFe_4O_x$ rod

Rod-like $CuFe_4O_x$ sample was prepared by the aqueous precipitation method which described detailed in the experiments. It is well known that the shape and phase composition of samples were intimately correlated to the synthesis conditions, like pH value, reaction time, calcination temperature. In the process of synthesis of rod-like $CuFe_4O_x$ precursor, $Na_2CO_3$ precipitant was introduced when the temperature increase to 120 ℃. It was found that the stirring time at 120 ℃ before $Na_2CO_3$ was introduced also effect the shape of product. As a result, we focus on the effect of pH value, stirring time at 120 ℃, calcination temperature on the shape and phase composition of $CuFe_4O_x$ sample.

Fig.1 shows the TEM images of precursors prepared under various pH values and stirring time at 120 ℃. In the experiment, yellow-brown precipitants were formed as $Fe^{3+}$ start to hydrolysis when temperature increased to 80~90 ℃. It is easy to understand the pH value of the system decreases with the hydrolysis of $Fe^{3+}$. While when the temperature continued rising to 120 ℃, $Fe^{3+}$ ions were completely hydrolyzed and the pH value of the solution was about 1 which is too low for $Cu^{2+}$ to form precipitant. It is obviously that the pH value was one of the most important factors. The pH value can be easily adjusted by adding different amount of $Na_2CO_3$. Fig.1(a, b, c) show the TEM images of precursors prepared at pH=12, 10 and 9, respectively. As pointed by the red arrow in

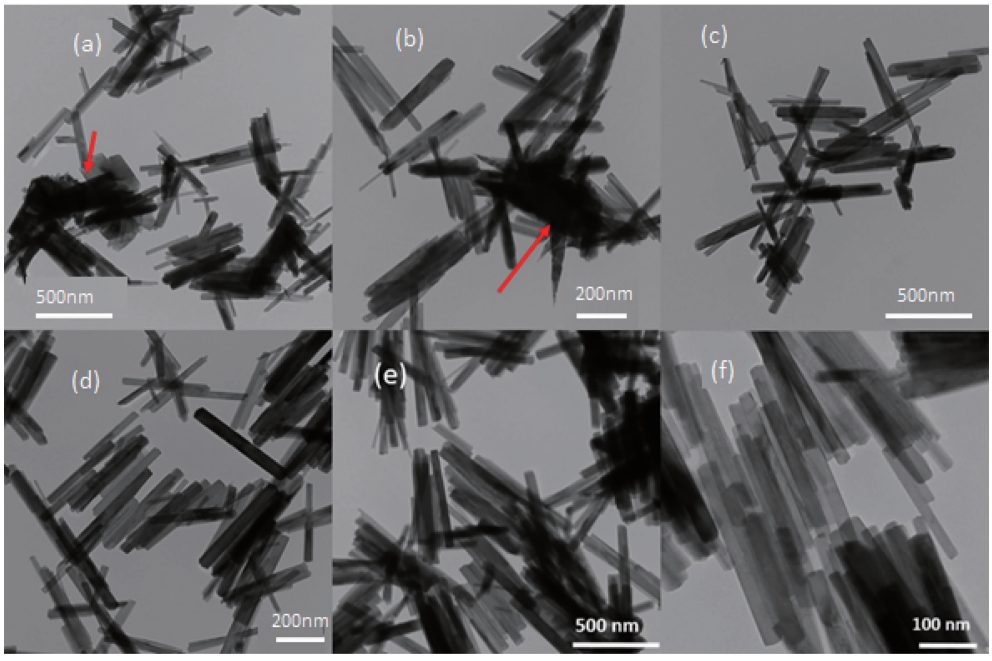


(a) pH=12, stirring time=0 h; (b) pH=10, stirring time=0 h; (c) pH=9, stirring time=0 h; (d) pH=9, stirring time=1 h; (e) and (f) pH=9, stirring time=3 h

Fig.1　TEM images of precursors prepared at different pH values and at 120 ℃ before $Na_2CO_3$ solution was introduced

Fig.1a and Fig.1b, that some nanoplates or spindle particles were formed besides rods when pH value is high to 10 or 12. While, when pH value was 9, only rod-shaped particles were detected in the products.

It has been reported that rod-shaped β-FeOOH was formed with the same aqueous precipitant method without $Cu^{2+}$ in the reaction system[14]. As a result, particles with plate or spindle shape (as shown in Fig. 1a and b) were attributed to the precipitant of $Cu^{2+}$. While when pH value was low to 9, only rod can be detected which means it is suitable for the preparation of rod-shaped sample when the pH value is 9. But the diameter and length of rods are not very uniform. It was found that the stirring time at 120 ℃ before $Na_2CO_3$ solution was introduced can also affect the uniform of rod shape. In order to obtain a rod-shaped sample with uniform diameter and length time-dependent experiments were carried out. When prolonging the stirring time at 120 ℃ before $Na_2CO_3$ solution was introduced, the diameter and length of the rod-shaped product become more and more uniform. When stirring time was extended to 3 h, more uniform rod-shaped precursors can be obtained as shown in Fig.1e and f. The average diameter and length of the rod-shape precursors are 30 and 285 nm, respectively.

Calcination is necessary for the formation of $CuFe_4O_x$ oxide composite. Fig.2 shows the XRD patterns of $CuFe_4O_x$ precursor before calcination and calcined at different temperatures for different time. It shows clearly that the uncalcined precursor was composed of β-FeOOH and CuO phases. When calcined at 500 ℃ for 5 h β-FeOOH transformed to α-$Fe_2O_3$ with that α-$Fe_2O_3$ reacted with CuO to form $CuFe_2O_4$ at the same time. While, CuO phase still can be detected by XRD which means CuO cannot completely reacted with $Fe_2O_3$ by calcination at 500 ℃ for 5 h. Prolong the calcination time to 10 h at 500 ℃, CuO phase was almost completely disappeared. However, when improved the calcination temperature to 600 ℃ and calcined for 5 h, CuO phase still can be detected. So, 500 ℃ is suitable to form $CuFe_2O_4$. Fig.3 shows the TEM images of samples obtained at different calcination conditions. It can be seen clearly that calcined at 500 ℃ for 5 h, sample can retain rod shape while when prolonged the time to 10 h at 500 ℃ or risen the calcination temperature to 600 ℃, sample was seriously sintered together. In order to obtain uniform rod shape, sample was calcined at 500

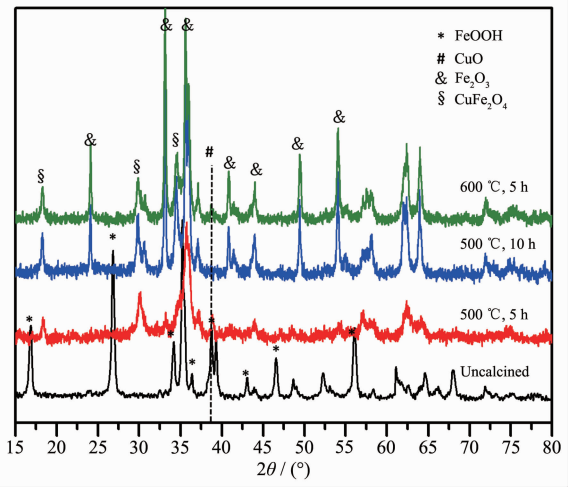


Fig.2 XRD patterns of uncalcined precursor and products obtained by calcined at different conditions

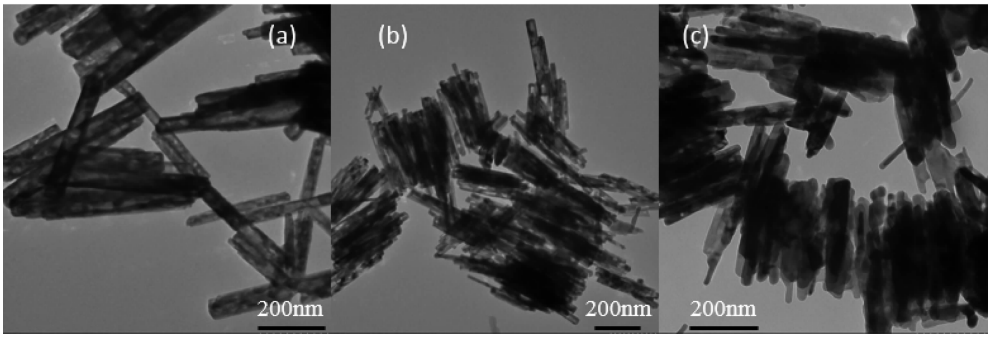


Fig.3 TEM images of $CuFe_4O_x$ samples obtained by calcination at different conditions: (a) 500 ℃ for 5 h; (b) 500 ℃ for 10 h; (c) 600 ℃ for 5 h

℃ for 5 h. ICP results of $CuFe_4O_x$ show that the ratio of Cu to Fe is consistent with the initial feed ratio which Cu versus Fe equal to 1:4. The BET surface area of $CuFe_4O_x$ which was calcined at 500 ℃ for 5 h was 36 $m^2 \cdot g^{-1}$. It is relatively high for metal oxide. From the TEM images (Fig.3a), it is clearly that a lot of pores are formed during the calcination. That is the reason why $CuFe_4O_x$ shows high BET surface areas.

### 2.2 Reducibility of the $CuFe_4O_x$ rod sample

In order to elucidate the surface and bulk oxygen reducibility of $CuFe_4O_x$ nanorods calcined at 500 ℃ for 5 h, $H_2$-TPR measurement was carried out and the TPR profile was shown in Fig.4. It presented two obviously different reduction regions: the low-temperature regime at 50~353 ℃ and the high-temperature regime at 353~650 ℃. As well studied that $Fe_2O_3$ shows one small peak at 420 ℃ for the reduction of $Fe_2O_3$ to $Fe_3O_4$ and one higher temperature peak above 650 ℃ for the reduction of $Fe_3O_4$ to metal Fe[15-16]. While $CuFe_2O_4$ also presents two distinct reduction peaks with one lower temperature reduction attribute to the reduction of $CuFe_2O_4$ to Cu and $Fe_3O_4$, and the other higher reduction peak assigned to the reduction of $Fe_3O_4$ to metal Fe[9]. It can be concluded that the reductions of Cu species and the reduction of $Fe_2O_3$ to $Fe_3O_4$ are much easier than the reduction of $Fe_3O_4$ to Fe. As a result, the lower peaks below 353 ℃ should be attributed to the reduction of $CuFe_2O_4$ to $Cu^0$ and $Fe_3O_4$ and the reduction of $Fe_2O_3$ to $Fe_3O_4$. The broad reduction peak around 530 ℃ should be assigned to the reduction of $Fe_3O_4$ to Fe metal as reported by Kameoka et al.[17] and Faungnawakij et al.[18]. It need to note that the small peak at 129 ℃ must be the reduction of surface $Cu^{2+}$ species, as only surface CuO can be reduced at such low temperature.

In order to get further insight about the phase transformation in the $H_2$ reduction process, the phases of $CuFe_4O_x$ were analyzed via *in-situ* XRD under 5% $H_2$ (He balance). Fig.5 shows the *in-situ* XRD evolution of $CuFe_4O_x$ rods under 5% $H_2$ (He balance) at different temperature. As mentioned before, the freshly prepared sample calcined at 500 ℃ for 5 h exhibits a phase mixture of $Fe_2O_3$ (PDF No.86-0550), CuO (PDF No.80-0076) and $CuFe_2O_4$ (PDF No.34-0425). It can be observed clearly that CuO and $Fe_2O_3$ are almost disappeared at 250 and 350 ℃, respectively, which suggests the reduction of $Fe_2O_3$ is more difficult than the reduction of CuO. The transformation of $CuFe_2O_4$ should happened at about 300 ℃ as the XRD reflection of $Cu^0$ suddenly increased. So, the spinel phase formed at temperature higher than 300 ℃ should be ascribed to $Fe_3O_4$ even though it is difficult to distinguish the XRD position of $Fe_3O_4$ and $CuFe_2O_4$. as $Cu^0$ was isolated from $CuFe_2O_4$. These analysis results support the ascription of TPR peaks at 129 ℃ to the reduction of CuO and the ascription of the

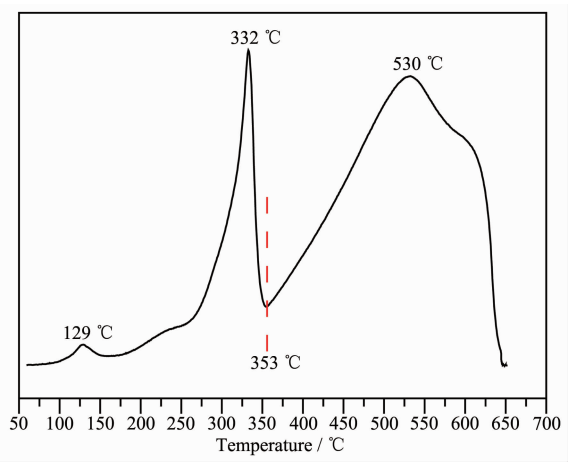


Fig.4 $H_2$-TPR profile of $CuFe_4O_x$ nanorods obtained by calcined at 500 ℃ for 5 h

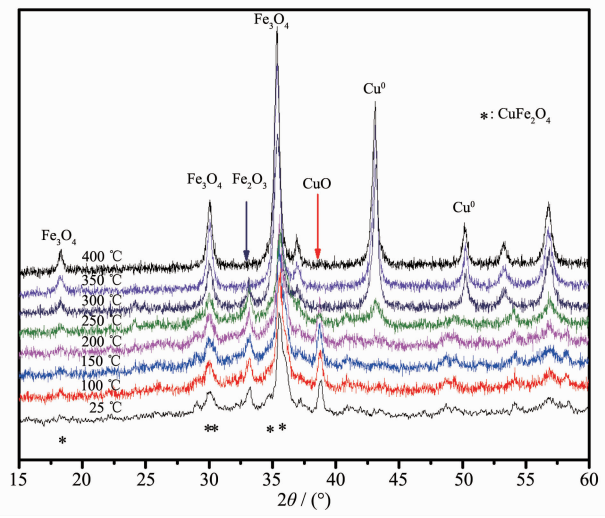


Fig.5 XRD patterns recorded *in-situ* during $CuFe_4O_x$ reduction under 5%$H_2$ (He balance) at different temperatures

following peak at 332 ℃ to the reductions of $CuFe_2O_4$ and $Fe_2O_3$. The broad reduction peak at 552 ℃ should be assigned to the reduction of $Fe_3O_4$ to $Fe^0$ as before.

### 2.3 Cu species of reduced sample

From the results of *in-situ* XRD and TPR analysis, it can be deduced that $CuFe_4O_x$ can be controllably reduced to Cu-$Fe_3O_4$. The TEM and HRTEM images of $CuFe_4O_x$ sample reduced at 300 ℃ are shown in Fig.6. Fig.6a and b display that $Fe_3O_4$ can inherit the rod shape of $CuFe_4O_x$ sample and a lot of nanoparticles are supported on the rod-particles. HRTEM results are shown in Fig.6c confirm the rod-shaped supports are $Fe_3O_4$ and supported small nanoparticles are $Cu_2O$. It is well known that freshly formed Cu nanoparticles are very active and can be oxidized when contact with air. As a result, the observed $Cu_2O$ nanoparticles must be the production of oxidation of Cu nanoparticles in air conditions. And the conclusion was further confirmed by the *in-situ* XPS results.

Fig.7 illustrates the XPS profiles of Cu2*p* and Cu$L_3VV$ of freshly prepared and *in-situ* reduced $CuFe_4O_x$ sample. For the freshly prepared $CuFe_4O_x$ sample, the kinetic energy of 917.5 eV in the spectra of Cu$L_3VV$ Auger corresponded to $Cu^{2+}$ [19]; the binding energy of Cu2$p_{3/2}$ at 932.9 eV, together with the relatively large satellite peak at 938~948 eV with a shake-up structure, further evidenced the presence of $Cu^{2+}$ [20-22]. Upon hydrogen reduction at 300 ℃, the shake-up satellite peak vanished, indicating the reduction of $Cu^{2+}$ species. The kinetic energy of 918.7 eV in Cu$L_3VV$ Auger spectra indicates the appearance of metallic copper species. Furthermore, the binding energy of Cu2$p_{3/2}$ in Cu2*p* spectra lowered to 931.9 eV representing metallic copper species. This result suggests the presence of $Cu^0$ after reduction at 300 ℃

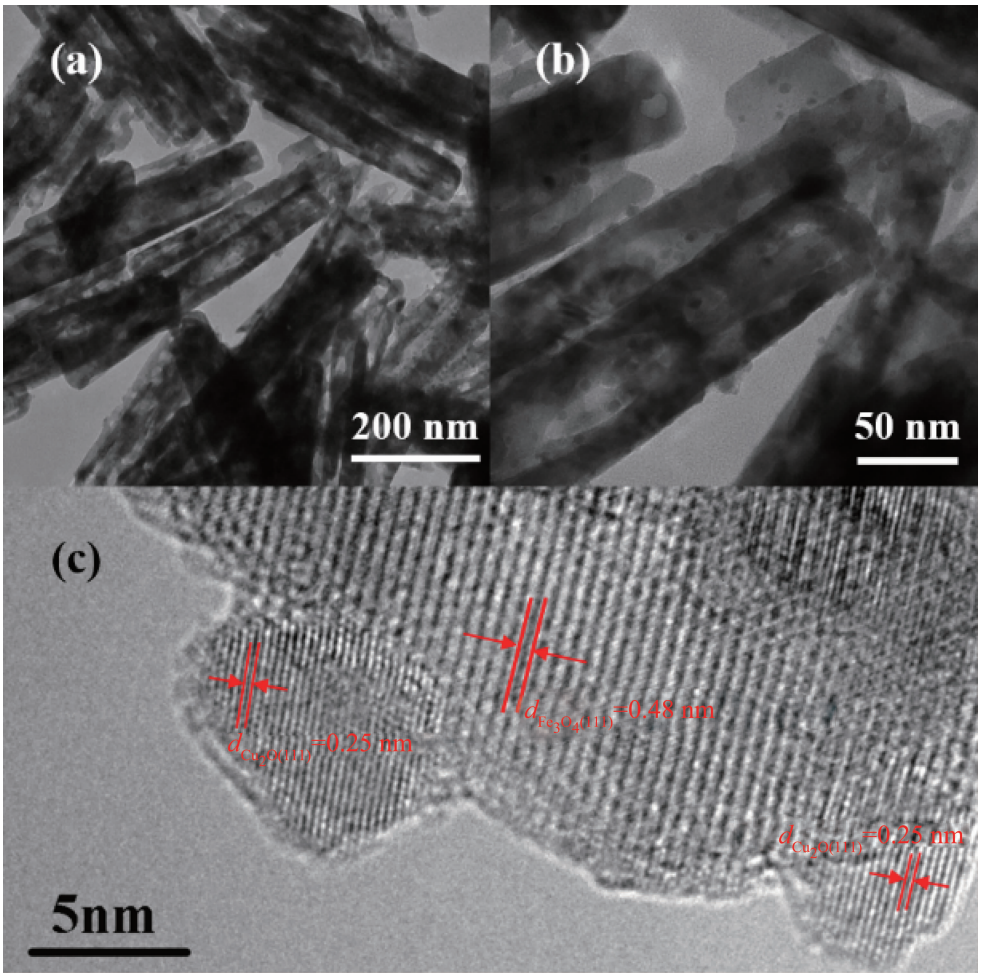


Fig.6 TEM (a, b) and HRTEM (c) images of the reduced $CuFe_4O_x$

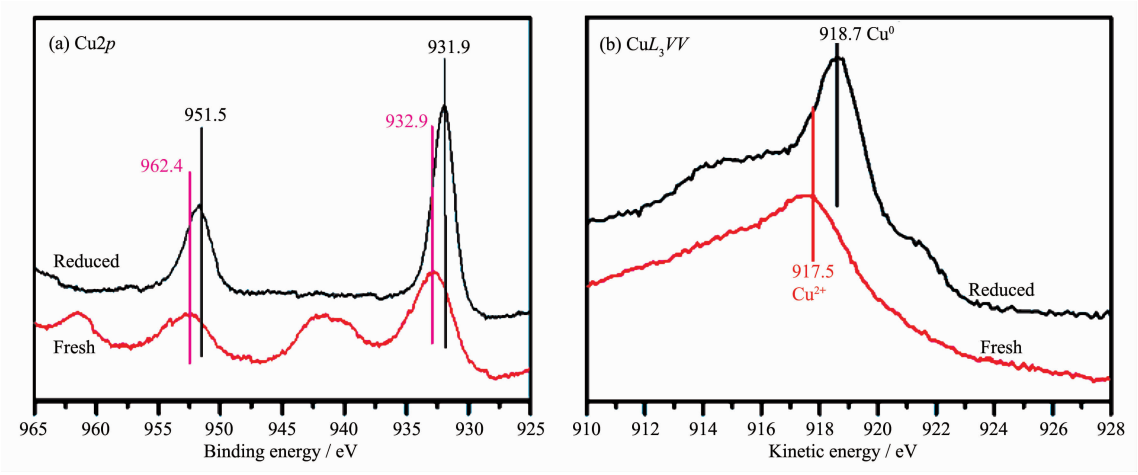


Fig.7　*In-situ* XPS profiles of reduced and fresh $CuFe_4O_x$ nanorods

in $H_2$. The combination of the results of *in-situ* XRD and *in-situ* XPS and HRTEM confirm that the $CuFe_4O_x$ samples are reduced to $Cu^0/Fe_3O_4$ rods composite by 5%$H_2$ at 300 ℃.

### 2.4　Dehydrogenation of isoamylic alcohol activity

It is known that copper based catalyst is used widely in the dehydrogenation of alcohols and copper is indeed an essential component of the active phase of the catalyst for the dehydrogenation of isoamylic alcohol. So, the catalytic activity of $CuFe_4O_x$ calcined at 500 ℃ and hydrogen reduced at 300 ℃ was assessed in the dehydrogenation of isoamylic alcohol to isovaleraldedyde. Co-precipitation method was used to prepare $CuFe_4O_x$ catalyst with same copper contents and its catalytic performance was compared with $CuFe_4O_x$ nanorods. ICP results show the molar ratio of copper to iron in both nanorods and nanoparticles are inconsistent with the formula of $CuFe_4O_x$. The TEM images and XRD patterns of reduced $CuFe_4O_x$ nanoparticles are shown in Fig.6a and 6b. The TEM image shows the sample was in the shape of nanoparticles and the XRD profile shows that nanoparticle is composed of well characterized $\alpha$-$Fe_2O_3$ and $CuFe_2O_4$ which shows the similar composition with nanorod samples.

Fig.8 shows the conversion versus time on stream using reduced $CuFe_4O_x$ catalysts with different shapes. It is clear that the initial conversion was similar for both nanoparticles and nanorods catalysts which illustrate that copper is the active phase for this reaction. However, there is a significant difference in their conversion profiles. The conversion of isoamylic alcohol over nanoparticles decreases rapidly to 0% in 500 min. While, the conversion over nanorods decreases to 40% at about 250 min and then the conversion can stable for more than 500 min. According to the catalytic analysis, it can be concluded that rod-shaped samples show higher stability than particles. The formation of this significant difference was thought to be the sintering of Cu particles or the formation of coke. As a result, the rod shape may increase the interaction of $Cu^0$ and $Fe_3O_4$ support and delay the growth of $Cu^0$ nanoparticles size.

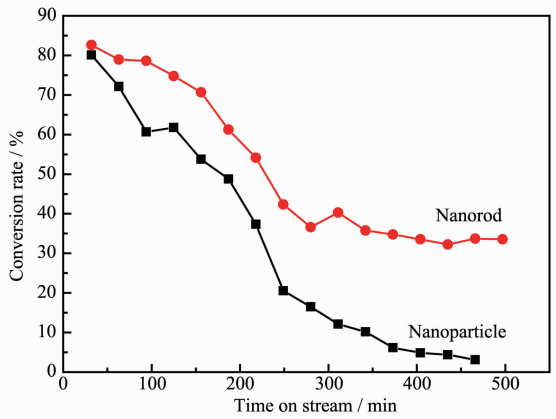


Reaction conditions: 300 ℃, $W/F_0$=41.3 $g_{catalyst}\cdot h\cdot mol^{-1}$ feed

Fig.8　Conversion rate of isoamylic alcohol vs time on stream using reduced $CuFe_4O_x$ nanoparticles and nanorods

## 3 Conclusions

In summary, we have prepared rod-shaped $CuFe_4O_x$ compound by one step liquid-phase precipitation method and the reaction conditions are carefully controlled. The structural analysis and reduction properties of $CuFe_4O_x$ have been performed. *In-situ* XRD and TPR analysis results show that Cu specie can be reduced at lower temperature than the reduction of $Fe_2O_3$ phase. When reduced at 300 ℃ by 5% $H_2$, $CuFe_4O_x$ can be reduced to $Cu^0/Fe_3O_4$ while $Fe_3O_4$ can inherit rod shape. The *in-situ* XPS and HRTEM results show that $Cu^0$ nanoparticles are highly dispersed on the surface of $Fe_3O_4$ rod. Comparing with $Cu/Fe_3O_4$ nanoparticles, $Cu/Fe_3O_4$ nanorods display higher stability in the dehydrogenation of isoamylic alcohol, suggesting that $Cu^0$ nanoparticles show better stability on rod-shaped $Fe_3O_4$ supporter.

**Acknowledgements:** This work is supported by the National Natural Science Foundation of China (Grant No. 21403124) and Natural Science Foundations of Shandong Province (Grants No.ZR2014JL014, ZR2014BM012).

## References:

[1] Li Y, Liu Q Y, Shen W J. *Dalton Trans.*, **2011**,**40**(22):5811-5826

[2] CAO Xiao-Feng(曹霄峰), ZHANG Lei(张雷), LI Zhao-Qian(李兆乾), et al. *Chinese J. Inorg. Chem.*(无机化学学报), **2012**,**28**(11):2373-2378

[3] HU Han-Mei(胡寒梅), DENG Cong-Hai(邓崇海), SUN Feng-Xia(孙凤霞), et al. *Chinese J. Inorg. Chem.*(无机化学学报), **2012**,**28**(2):405-410

[4] Ratnasamy C, Wagner J P. *Catal. Rev. Sci. Eng.*, **2009**,**51**(3):325-440

[5] Gawande M B, Goswami A, Felpin F, et al. *Chem. Rev.*, **2016**,**116**(6):3722-3811

[6] DING Ying-Ru(丁莹如), YAO Jian-Hua(姚建华), LIU Qi-Sheng(刘其盛), et al. *Chinese J. Inorg. Chem.*(无机化学学报), **1989**,**5**(1):119-121

[7] Estrella M, Barrio L, Zhou G, et al. *J. Phys. Chem. C*, **2009**, **113**(32):14411-14417

[8] Takeguchi T, Kani Y, Inoue M, et al. *Catal. Lett.*, **2002**,**83**(1/2):49-53

[9] Yang S C, Su W N, Lin S D, et al. *Appl. Catal., B*, **2011**, **106**(3/4):650-656

[10]Kameoka S, Tanabe T, An P T. *Catal. Lett.*, **2005**,**100**(1/2):89-93

[11]Carotenuto G, Tesser R, Serio M D, et al. *Catal. Today*, **2013**,**203**(203):202-210

[12]Shiau C Y, Chen S, Tsai J C, et al. *Appl. Catal., A*, **2000**, **198**(1/2):95-102

[13]Crivello M, Pérez C, Fernández J, et al. *Appl. Catal., A*, **2007**,**317**(1):11-19

[14]Mou X L, Zhang B S, Li Y, et al. *Angew. Chem. Int. Ed.*, **2012**,**51**(12):2989-2993

[15]Khan A, Smirniotis P G. *J. Mol. Catal. A*: *Chem.*, **2008**,**280**(1/2):43-51

[16]Reddy G K, Gunasekera K, Boolchand P, et al. *J. Phys. Chem. C*, **2011**,**115**(15):7586-7595

[17]Kameoka S, Tanabe T, An P T. *Appl. Catal., A*, **2010**,**375**(1):163-171

[18]Faungnawakij K, Kikuchi R, Fukunaga T, et al. *Catal. Today*, **2008**,**138**(3/4):157-161

[19]Poulston S, Parlett P M, Stone P, et al. *Surf. Interface Anal.*, **1996**,**24**(12):811-820

[20]Tang X, Zhang B, Yong L, et al. *Appl. Catal., A*, **2005**,**288**(1/2):116-125

[21]Zeng S H, Liu K W, Zhang L, et al. *J. Power Sources*, **2014**, **261**(5):46-54

[22]Qi L, Yu Q, Dai Y, et al. *Appl. Catal., B*, **2012**,**119-120**(21):308-320